EASR

Engineering and Applied Science Research

https://www.tci-thaijo.org/index.php/easr/index

Published by the Faculty of Engineering, Khon Kaen University, Thailand

Experimental and modeling studies of methylene blue adsorption onto Na-Bentonite clay

Channarong Puchongkawarin*, Supatpong Mattaraj and Chakkrit Umpuch

Department of Chemical Engineering, Faculty of Engineering, Ubon Ratchathani University, Ubon Ratchathani 34190, Thailand

Received 22 April 2020
Revised 27 July 2020
Accepted 23 September 2020

Abstract

This study aimed to investigate methylene blue (MB) adsorption onto Na-bentonite as adsorbent. Individual effects of operating factors including initial MB concentration, pH, contact time and temperature on the performance of adsorption were firstly investigated. Results showed that these factors had significant effects on adsorption of MB solution. The adsorption rate was rapid at the initial stage and it reached equilibrium in a few minutes. For kinetic and equilibrium studies, pseudo-first, pseudo-second order and Langmuir models were able to fit experimental data with the maximum adsorption capacities ranging from 398.28 - 465.28 mg/g. Also, thermodynamic studies showed that the process under study was the spontaneous and endothermic reaction. Finally, the surrogate-based model was developed to study interaction effects of operating factors and to examine the optimal condition. The optimal conditions for this study were found at the initial concentration of 634 mg/L, a pH of 10, and a temperature of 55°C.

Keywords: Adsorption, Surrogate-based models, Langmuir isotherm, Optimization, Kinetics, Thermodynamics

1. Introduction

Several sectors such as food, textile, and leather, etc. have used dyes to color products [1]. Now, over 0.7 million tons of dyes are produced annually and certain quantities of the total dyes (5-10%) are discharged into the water body as industrial effluent [2, 3]. It is widely known that contamination of dyes in water can be a major problem due to the negative impact on a wide variety of lives, so the discharge of water containing dyes can have impacts on toxicological and esthetical aspects [4]. In addition, most dyes are slightly biodegradable, and cannot be removed by using conventional approaches. Almost 90% of reactive dyes remain the same after passing through a wastewater treatment plant [5]. One example of a dye substance typically used for coloring products, e.g. cotton, silk, and wood is methylene blue (MB) [6]. Even though MB has been applied to several industries, it potentially causes eye burn, permanent eye injury [7], nausea, vomiting, diarrhea, gastritis, profuse sweating, mental confusion, and breathing difficulties upon inhalation [7, 8]. To avoid these problems, dye wastewater needs proper treatment approaches before discharge to the environment.

A number of approaches have been developed to decolorize dye wastewater including biological, chemical and physical methods [9], but only a few approaches have been widely adopted to industries. Adsorption is, however, among treatment methods which demonstrate the potential for removing different kinds of color substances [10]. The basic concept of adsorption is that undesired substances are moved from the water solution to a solid adsorbent which can be regenerated to be reused, kept in place without affecting the environment or eliminated using environmentally friendly approaches. Activated carbon (AC) as an adsorbent has been widely used for eliminating dyes from wastewater thanks to its properties which are suitable for adsorption [11]. However, the use of AC in the large-scale processes is limited because it is expensive [12]. Many studies have focused on a low-cost material [13-17]. Clay minerals such as bentonite and its activated form have been extensively used as adsorbents for removing the dye from wastewater, thanks to their high specific surface areas and cation exchange capacities. These clay minerals have more advantages in terms of abundance in nature and availability at lower cost [17, 18]. In addition, several manufacturers and suppliers of clay minerals are available in Thailand so it is more convenient to use as an adsorbent, because these clay minerals are in a ready to use form through the purification process. In this study, Na-bentonite is chosen as the adsorbent since it possesses net negative surface charge so it is likely for MB or a positively charged blue dye to bind to the negatively charged surface of Na-bentonite.

Regarding MB removal using bentonite and activated bentonite such as Na-bentonite, effects of operating factors have already been investigated by several studies [19-23]. The common approach to investigating these effects is to change an operating factor while fixing other operating factors constant. This can describe the effects of operating factors individually but it is inadequate to describe the interaction of such operating factors or the relationship among operating factors. Apart from this, the effects of operating factors, selection of the optimal operating condition is another important aspect that needs to be taken into consideration for process operation. To study the interaction effects of operating factors and choose the optimal condition, surrogate-based modeling is commonly used. It is a mathematical approximation technique used for improving and optimizing the process. It is also used to transform the complex process into the mathematically simple model or the input-output relationships of the complex process. It has been used in many aspects in chemical engineering domain such as simplifying unit operation, identifying the feasible region of unit operation, and process optimization to improve capability and performance

*Corresponding author. Tel.: +66 4535 3343
Email address: channarong.p@ubu.ac.th
doi: 10.14456/easr.2021.29

[24, 25]. This method involves planning to collect appropriate data, analyzing the collected data, and selecting the suitable model to represent the input/output relationship. Consequently, it can result in a reliable and valid conclusion. The main contribution in this work is to study the effects of operating factors individually on adsorption of MB using Na-bentonite as an adsorbent including initial MB concentration, contact time, initial pH, and temperature. The pseudo-first and second order kinetics are also analyzed to investigate kinetic parameters of MB removal using Na-bentonite. Then, equilibrium information is evaluated using Langmuir as well as Freundlich models and adsorption thermodynamics will be analyzed. Additionally, the interaction effects of operating factors and optimization are studied based on the surrogate-based model.

Although Na-bentonite has been studied extensively for dye adsorption, there is still research potential for improving the adsorption performance and identifying the relationship between its performance and operating factors. The key finding in this study would be beneficial from technical point of view because it can be used to explain interaction between operating factors and determine the optimal operating conditions for the removal of MB. Also, it can be a reference for wastewater treatment produced from local textile industries.

2. Materials and methods

2.1 Chemicals and clay

MB solution was used as adsorbate and its molecular formula is $C_{16}H_{18}N_3SCl \cdot 3H_2O$ with molecular weight (MW) of 319.85 g/mol. MB was purchased from the Asia Pacific Specialty Chemical company. Stock of MB with concentration of 1 g/L was prepared in distilled water, and then diluted to obtain the desired MB concentration. Na-bentonite as an adsorbent was purchased from the Supsuwan industry company (Thailand).

2.2 Characteristics and analysis

An ultraviolet-visible spectrophotometer (UV/VIS) was used to analyze MB concentration through a calibration curve which shows the relationship between MB concentrations and absorbance.

The Na-bentonite characteristics were analyzed by X-ray fluorescence (XRF) as well as a scanning electron microscope (SEM) to evaluate chemical composition and surface of morphology. Also, a spectrum Fourier transform infrared (FT-IR, FTIR2000) spectroscopy with a frequency number ranging from 4,000 to 400 cm^{-1} and X-ray diffraction (XRD, X' Pert Phillips) in the 2θ angle ranging from 5° to 90° with the scan rate of 0.04 degree per minute were used to investigate functional groups and lattice spacing, respectively. BET surface area and pore diameter of the Na-bentonite were determined by N_2 adsorption/desorption at 77 K using an automatic surface analyzer (Quanta chrome Instrument, ASI-C-8).

2.3 Batch tests

Initially, 100 mL of MB solutions with concentrations of 100-700 mg/L were prepared in 200 mL conical flasks. After that 0.1 g of Na-bentonite was added into the solutions to adsorb the MB molecules. The flasks were then shaken in the incubator shaker at a constant speed of 200 revolutions per minute (rpm) for centrifugation with different control temperatures (35-55°C) for 120 minutes. After shaking the conical flasks, MB adsorbed Na-bentonite was separated from the solutions by means of centrifugation. Finally, the concentration of supernatant was measured using a UV/VIS spectrophotometer (λ_{max} = 615 nm) to detect the remaining amount of MB in the solutions. Adsorption capacity of Na-bentonite or the amount of MB adsorbed onto Na-bentonite at time t was determined by the following equation:

$$q_t = \frac{(C_0 - C_t)V}{m} \quad (1)$$

where q_t represents the adsorption capacity of Na-bentonite (mg/g) at time t; C_0 and C_t are the initial MB concentration and MB concentration at any time t, respectively (mg/L); V is the volume of MB solution (L), and m is a unit mass of Na-bentonite (g). Performance of MB removal using Na-bentonite can also be indicated using percent removal as given by:

$$\%\text{Removal} = \frac{(C_0 - C_e)}{C_0} \times 100 \quad (2)$$

where C_0 and C_e are initial and equilibrium concentrations of MB solution. Note that, a similar approach was conducted at equilibrium (contact time > 120 minutes was used to make sure that it reached equilibrium) with various initial MB concentrations.

2.4 Development of surrogate-based models

A surrogate-based model is known as the approximation or mathematically simple model used for mapping input-output relationships of complex systems or processes. It has been used in several engineering practices and applications [24, 25]. It is developed from samples or experimental data obtained by the design space. Note that the quality of surrogate-based models depends on a sampling data point and there is no rigorous way for sampling methods. Generally, design of experiment (DOE) is used to evaluate sample points in the design space with the purpose of maximizing the amount of information obtained from limited sample points. Once experimental data at the sampling data point is collected, surrogate-based models are developed. There are several techniques used to develop surrogate-based models such as Kriging, and radial basis functions. The polynomial respond surface model (RSM) is one of the common methods for developing surrogate-based models. The main advantage of this technique over other methods is that it is computationally simple and convenient to evaluate information from the magnitude of coefficients. The general mathematical model of sampling data is given as:

$$y(x) = \hat{y}(x) + \varepsilon, \quad x \in \mathbb{R}^m \quad (3)$$

where $y(x)$, $\hat{y}(x)$ are the sampling/experimental data and the response of surrogate-based models, respectively. ε is errors or gaps between model prediction and experimental data. The response of the surrogate-based model can be defined as:

$$\hat{y}(x) = \beta_0 + \sum_{i=1}^{m} \beta_i x_i + \sum_{i=1}^{m} \beta_{ii} x_i^2 + \sum_{i=1}^{m} \sum_{j \geq i}^{m} \beta_{ij} x_i x_j \quad (4)$$

where β_0, β_i, β_{ii}, β_{ij} are constant, linear, quadratic and cross-product coefficients, respectively; x_i, x_j are independent factors. After a surrogate-based model is developed, it needs to be validated using different sampling data points or different sets of experimental data to ensure its applicability. It is important to point out that the development of surrogate-based models is repeatedly performed from sampling data points to improve model accuracy until the stopping criteria are met. The validated surrogate-based model is then used for predicting or optimizing complex processes. Note that there is always a trade-off between computational expense and model accuracy. For example, the higher-order polynomial models usually provide a better fit than the linear models but the non-linear models are more complex to develop and use.

In this study, the interaction effects of operating factors and the optimal operating conditions were investigated through the surrogate-based model. Full factorial design experiments were performed to analyze performance of the adsorption process in

Table 1 Level of operating factors.

Operating factors	Low level (-1)	Mid-level (0)	High level (+1)
Temperature (°C), x_1	35	45	55
pH, x_2	2	6	10
Initial concentration (mg/L), x_3	100	400	700

Table 2 Chemical composition of Na-bentonite.

Chemical composition	Percent (%)	Chemical composition	Percent (%)
SiO_2	61.59	MgO	1.47
Al_2O_3	15.37	CaO	1.22
Fe_2O_3	6.19	Na_2O	2.07
TiO_2	1.08	K_2O	0.43
MnO	0.04	P_2O_5	0.06

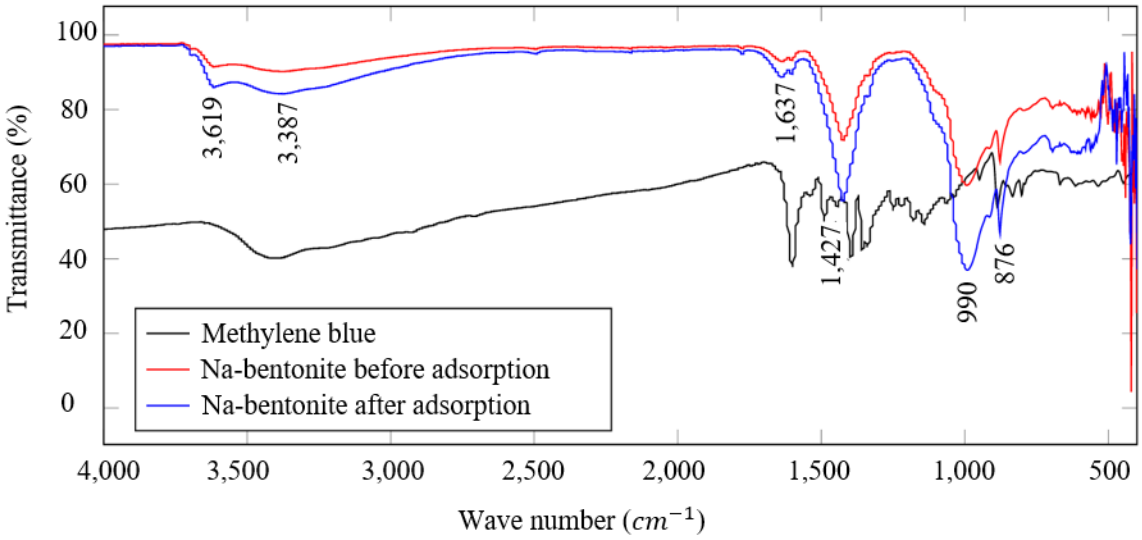

Figure 1 FTIR Spectra of Na-bentonite

terms of adsorption capacity at equilibrium or the amount of MB adsorbed onto Na-bentonite at equilibrium. Three factors with three levels were studied including initial MB concentration, initial pH, and temperature as presented in Table 1. Then, a surrogate-based model was developed using the polynomial RSM to provide a better understanding of interactive effects. After that, the surrogate-based model was validated using different sets of experimental data by comparing the prediction of the surrogate-based model and experimental data. Finally, the validated surrogate-based model was used to optimize the operating condition of MB adsorption onto Na-bentonite.

3. Results and discussions

3.1 Characterization of Na-bentonite

The chemical composition of Na-bentonite from XRF analysis is shown in Table 2. SiO_2 and Al_2O_3 were apparently major components of Na-bentonite accounting for 76.96% with the ratio of 4:1. The ratio was almost twice as high as the theoretical value of perfect montmorillonite (2.6:1) [20] indicating a relatively high content of SiO_2 and it was claimed that the SiO_2 compound could be used as an adsorbent for simple molecules and ions [26]. Additionally, the higher percentage of Na_2O compared to CaO and K_2O allowed us to classify the interlayer cation in montmorillonite into Na-bentonite as shown in Table 2.

The BET surface area, pore volume and pore diameter were obtained from N_2 adsorption/desorption isotherms at 77 K. The results showed that the N_2-BET surface area and total pore volume for pores were 77.55 m^2/g and 0.1044 cm^3/g, respectively. Also, the average pore diameter of Na-bentonite was 42.96 nm. Typically, bentonite has surface area, total pore volume and average diameter in the range of 27-57 m^2/g, 0.09 - 0.13 cm^3/g and 2.34-11 nm, respectively, which have been reported in some previous works [27, 28].

To investigate functional groups of Na-bentonite, FTIR spectra of Na-bentonite before and after adsorption were analyzed and the result is shown in Figure 1. The FTIR analysis on the Na-bentonite before MB adsorption showed the absorption band was detected at 3,619.49 cm^{-1} [υOH] representing the stretching vibration of AlOH and SiOH which can be attributed to the OH group of Na-bentonite. The board band at 3,387.23 cm^{-1} [υOH] represents stretching vibration of OH for hydrogen bonds. The bands at 1,637.89 cm-1 [υHOH] to bending vibration of OH, 1,427.87 cm^{-1} [υSiO] to the stretching vibration of SiO, 990.53 cm^{-1} [υAlAlOH] to the bending vibration of AlAlOH, and 876.87 cm^{-1} [υCO] to the stretching vibration of CO were also detected [29-31]. After MB adsorption, the spectrum of MB loaded adsorbent was mostly the same as that observed in the MB free adsorbent and only the intensity of the peaks changed. On the contrary, the FTIR spectrum of MB (black line in Figure 1) shows more complicated vibration peaks. Some of these peaks did not appear in the FTIR spectra of the MB loaded adsorbent and possibly contributed to the intensity of the peaks. Significant changes in the peak intensity indicate the existence of physical interaction between the adsorbent and the MB. The similar result was found in the study of Xu et al. [32] and Ainane et al. [33].

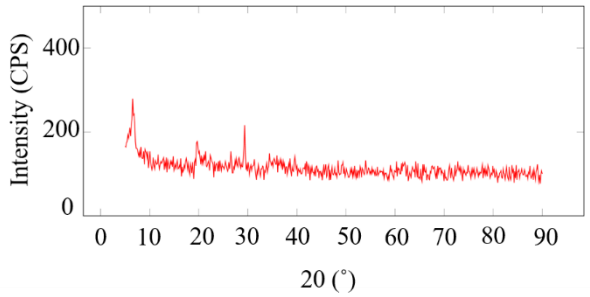

Figure 2 XRD Pattern of Na-bentonite.

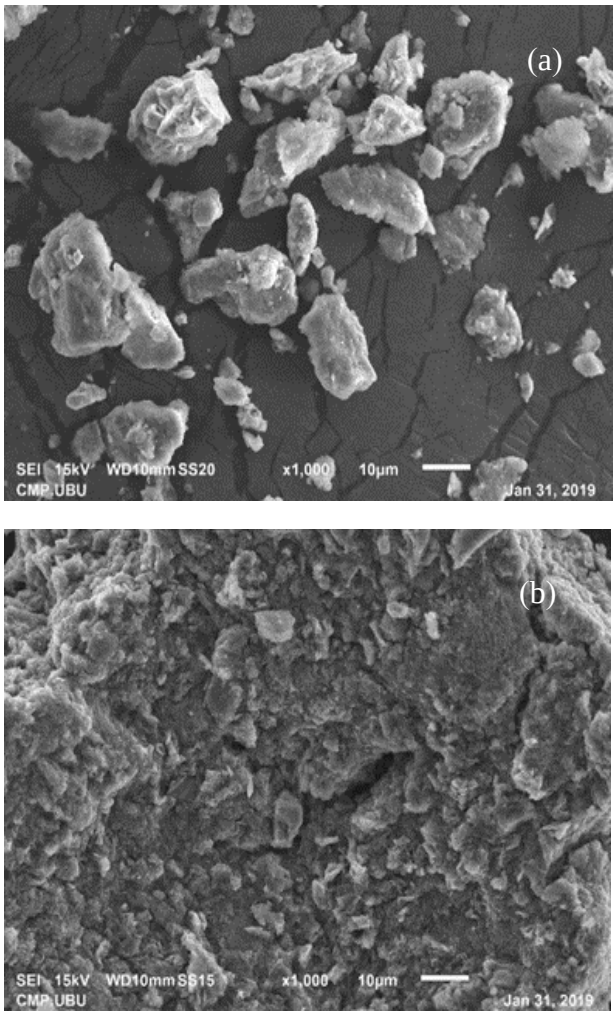

Figure 3 SEM Images of Na-bentonite (a) before adsorption (b) after adsorption at 1,000 magnification.

Figure 2 shows the XRD pattern of Na-bentonite and the diffraction peaks were detected at $2\theta = 6.55^{o}$ and 29.37^{o} corresponding to a basal spacing)d001 (of 13.49 A and 3.04 A, respectively this reflects that the surface of Na-bentonite has a lattice structure consisting of montmorillonite and quartz with characteristic features .The other peaks correspond to impurities [34].

The morphological structure of Na- bentonite was investigated by using SEM at 1,000 magnification before and after MB adsorption. It was found that their surface morphologies were obviously different. Figure 3(a) shows the SEM image of Na-bentonite before adsorption and abundant pores distributed on the surface. These pores allowed MB molecules to diffuse into the interior of Na-bentonite when it was immersed with MB solution. Also, its superficial area before adsorption was large

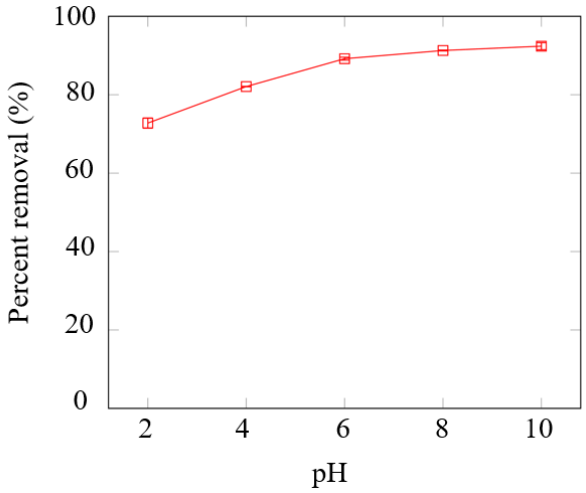

Figure 4 Effect of pH on adsorption capacity at equilibrium.

and the lamellar structure stacked together. Figure 3(b) shows the Na- bentonite surface after adsorption. The surface of Na-bentonite became tighter and space between layers of Na-bentonite was reduced. This is possibly because the MB solution was adsorbed on the surface.

3.2 Effect of operating factors

3.2.1 Initial pH

The initial pH of the solution can influence the adsorption capacity in terms of the degree of ionization and surface properties of the adsorbent [35]. In this section, the effect of initial pH ranging from 2-10 on the adsorption capacity at equilibrium was investigated while the initial MB concentration, temperature, and contact time were fixed at 400 mg/L, 35°C, and 120 minutes, respectively. The initial pH of MB solution was adjusted by sodium hydroxide (NaOH)/hydrochloric acid (HCl) and the adjusted pH was measured using the pH meter. Figure 4 shows percent removal of the MB adsorption using Na-bentonite at various initial pH values. It was obvious that adsorption of MB solution onto Na-bentonite depended on the initial pH as the percent removal of MB solution increased significantly from 73% to 89% with an increase in the initial pH from 2 to 6. At the initial pH above 6, the percent removal of MB solution increased slightly from 89% to 92%. The favorable adsorption and the maximum percent removal of MB solution were found at the high pH of 10. The possible reason is that the performance of MB adsorption is influenced by surface charges on the adsorbent and MB as a cationic dye which is available in the form of positively charged ions. At the lower initial pH, the excess H^{+} from protonation and MB molecules are competitively adsorbed on the free adsorbent sites. This can consequently decrease the possibility of MB molecules adsorbed onto the adsorbent. Conversely, an increase in the initial pH decreases the competing H^{+}, yielding a favorable outcome for the MB adsorption onto Na-bentonite. The results yielded a similar trend to the study of Liu and Zhou [36] investigating removal of Ni and Cu using Na-bentonite at different pH. The percent removal of Ni and Cu on Na-bentonite increased with an increase in pH. Additionally, pH point of zero charge (pH_{pzc}) was determined to indicate the type of surface-active centers [37] and to provide better understanding of adsorption mechanisms. The result showed that pH_{pzc} was found to be 2. At $pH > pH_{pzc}$, the surface has net negative charges and it is favor for MB (cationic dye) adsorption because functional group such as OH^{-} is presented [38].

3.2.2 Contact time

The effect of contact time is another factor for the adsorption process in terms of both adsorption capacity and economic aspects. The effect of contact time at 0-120 minutes on the adsorption capacity was investigated while other operating factors were kept constant (pH = 10, initial concentration = 400 mg/ L, temperature = 35ºC). Figure 5 shows the adsorption capacity of MB solution at different times. Rapid adsorption occurred at the initial stage of the contact time observed from the high adsorption capacity and it reached equilibrium in a short time. This can be explained by a large number of active sites being occupied by MB molecules and this leads to the high adsorption rate at the initial stage. Then, MB removal kept constant where no more MB molecules were removed. The rapid equilibrium may result from the fact that the number of MB molecules mainly adsorbs on the external surface of the Na-bentonite and then the adsorbed MB molecule form a layer as displayed in Figure 3(b) which could be a barrier for the MB transferring into the interior of the adsorbent.

3.2.3 Temperature

Another important factor affecting MB adsorption is temperature because it has been proved by several studies that temperature can change the adsorption capacity [7]. The effect of temperature on the adsorption of MB solution using Na-bentonite was investigated by varying temperatures from 35 to 55ºC while the initial concentration, contact time and initial pH were kept constant at 400 mg/ L, 120 minutes, and 10, respectively. The effect of temperature on the MB adsorption onto Na-bentonite is shown in Figure 6. It appeared that the effect of temperature on the adsorption of MB solution onto Na-bentonite. It was found that the adsorption capacity slightly increased from 340 to 370 mg/L when the temperature was raised from 35 to 55ºC. It is believed that varying the temperature can consequently change the equilibrium capacity of the adsorbent for some particular adsorbates [39]. Also, an increase in temperature may decrease resistance of the boundary layer as presented in Figure 3(b) so the higher amount of MB is able to diffuse to internal pores. From the results, it can be seen that the MB adsorption on Na-bentonite is an endothermic process.

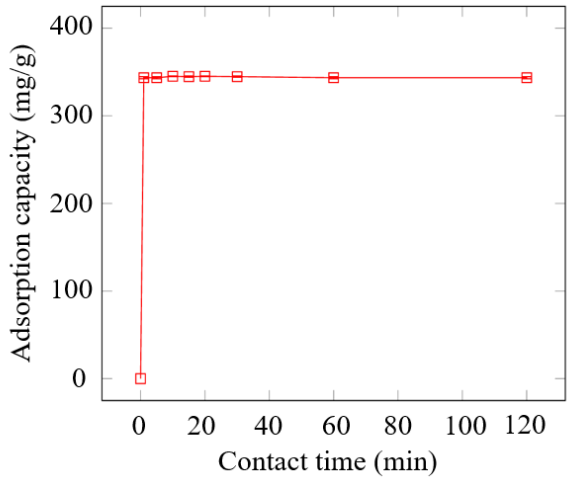

Figure 5 Effect of contact time on adsorption capacity at equilibrium.

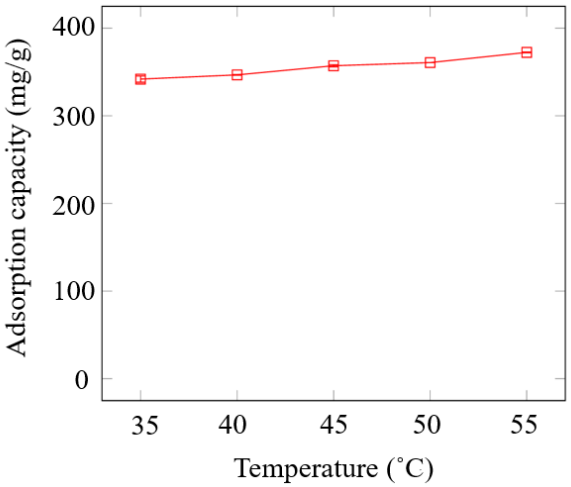

Figure 6 Effect of temperature on adsorption capacity at equilibrium

3.2.4 Initial MB concentration

To study the effect of initial MB concentrations on the adsorption capacity, experiments were performed at different initial MB concentrations (100-700 mg/ L) while keeping operating factors constant (pH = 10, temperature = 35ºC, contact time = 120 minutes). Figure 7 shows the effect of initial MB concentrations on the adsorption capacity at equilibrium. It appeared that the initial MB concentration affected and played an important role in the adsorption capacity of MB. As the initial MB concentration increased from 100 to 500 mg/ L, the adsorption capacity increased from 97 to 400 mg/ g. This is possibly because the larger difference between the concentration of MB solution and solid phase can be the driving force to overcome resistances between MB solution and the solid phase [40]. However, the adsorption capacity started decreasing when the initial MB concentration became greater than 500 mg/L. This is due to the fact that the adsorbent has a limited number of active sites and it may be saturated at a certain concentration of MB solution. Overall, the adsorption capacity increases with an increase in the initial MB concentration (100-500 mg/L) because of the concentration gradient between MB solution and Na-bentonite leading to the larger driving force for the mass transfer. At a certain concentration, the initial concentration has an inverse effect on the adsorption capacity because of the limited number of active sites for adsorption. A similar trend was also observed from the adsorption of dye solution on activated carbon [41].

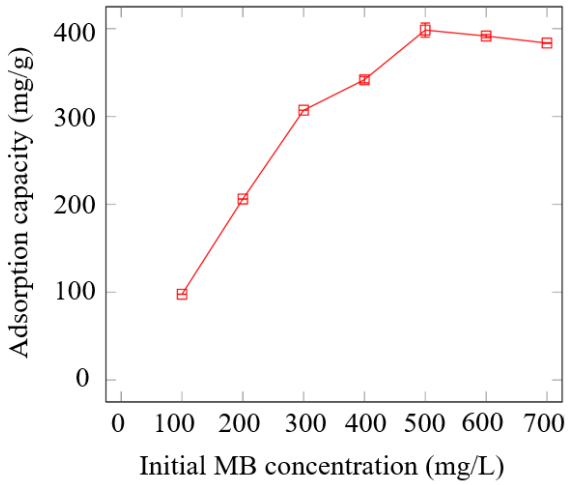

Figure 7 Effect of initial MB concentrations on adsorption capacity at equilibrium.

Table 3 Kinetic parameters of pseudo-first and second order reactions for adsorption of MB onto Na-bentonite.

T (°C)	$q_{e,exp}$ (mg/g)	Pseudo-first order			Pseudo-second order		
		$q_{e,pre}$ (mg/g)	K_1 (1/min)	χ^2	$q_{e,pre}$ (mg/g)	K_2 g/(mg·min)	χ^2
35	343.53	344.34	6.06	0.01	344.39	1.16	0.01
40	346.74	347.11	6.85	0.007	347.13	2.86	0.007
45	357.16	357.31	7.8	0.004	357.3	10.00	0.004
50	360.77	360.76	19.83	0.002	360.78	9.05	0.002
55	372.39	372.78	6.89	0.006	372.77	4.45	0.006

3.3 Kinetic studies

Kinetic studies of MB adsorption onto Na- bentonite are important because they are used to identify operating conditions for batch processes. Parameters obtained are used for predicting the adsorption rate, and providing information for design and modeling purposes. In this study, two kinetic models were investigated to study mechanisms of the adsorption process: pseudo- first order and pseudo- second order models. Note that linear regression is commonly used to determine the best fit for kinetic models. However, adsorption kinetics require linearization to determine model parameters. It was reported that the transformation of non-linear equations into linear forms may change the error structure in the measurement of parameters. Non- linear curve fitting is another mathematical method used to calculate model parameters. Recently, this approach has been the center of focus and can be superior to linear regression because parameters are not distorted during the transformation of non-linear forms into linear forms. There is also no need to know q_e prior to fitting the experimental data [42, 43].

The pseudo- first- order model can be used to describe the adsorption rate through adsorption capacity expressed as follows [44]:

$$\frac{dq_t}{dt} = K_1(q_e - q_t) \quad (5)$$

Where q_t and q_e are adsorption capacity (mg/ g) at time t and equilibrium, respectively. K_1 is the rate constant (min^{-1}) . Integration of Eq. (5) with respect to boundary conditions results in the following equation:

$$q_t = q_e(1-e^{-K_1 t}) \quad (6)$$

Kinetic studies were also investigated using a pseudo- second order model. Generally, differential equation of the pseudo-second order model can be described as [45]:

$$\frac{dq_t}{dt} = K_2(q_e - q_t)^2 \quad (7)$$

Where K_2 is the rate constant (g/ mg· min) . Once Eq. (7) is integrated using boundary conditions, a non- linear relationship can be obtained:

$$q_t = (K_2 q_e^2)t/(1+K_2 q_e t) \quad (8)$$

In order to determine the best parameters, minimization of error function (χ^2) was used as given by:

$$\chi^2 = \sum_{i=1}^{N} \frac{(q_{t,exp} - q_{t,pre})^2}{q_{t,pre}} \quad (9)$$

Where N is the number of experimental data, $q_{t,exp}$ and $q_{t,pre}$ are adsorption capacity (mg/g) obtained from experiments and kinetic models. The value of χ^2 is expectedly close to 0 indicating that the calculated adsorption capacity obtained from models is close to the experimental data [46, 47] . The kinetic parameters, K_1, K_2, q_e and χ^2 of the pseudo-first order and the pseudo-second order models are presented in Table 3. It was found that χ^2 values of the pseudo- first order models were close to 0 and the corresponding plot of the pseudo- first order model is presented in Figure 8(a) . This implies that the pseudo- first order model provided good agreement with experimental data. Similarly, the prediction using the pseudo- second order model showed good compliance with the experimental data since the χ^2 values obtained from linear regression were close to 0. The corresponding plot of the pseudo- second order models is presented in Figure 8(b). It becomes clear that the kinetics of MB adsorption onto Na-bentonite follows both the pseudo-first order and pseudo- second order rate. This indicates that the formation of MB and the adsorbent interactions at the external surface of adsorbent are a rate of limiting step and the adsorption is of a chemical nature [48].

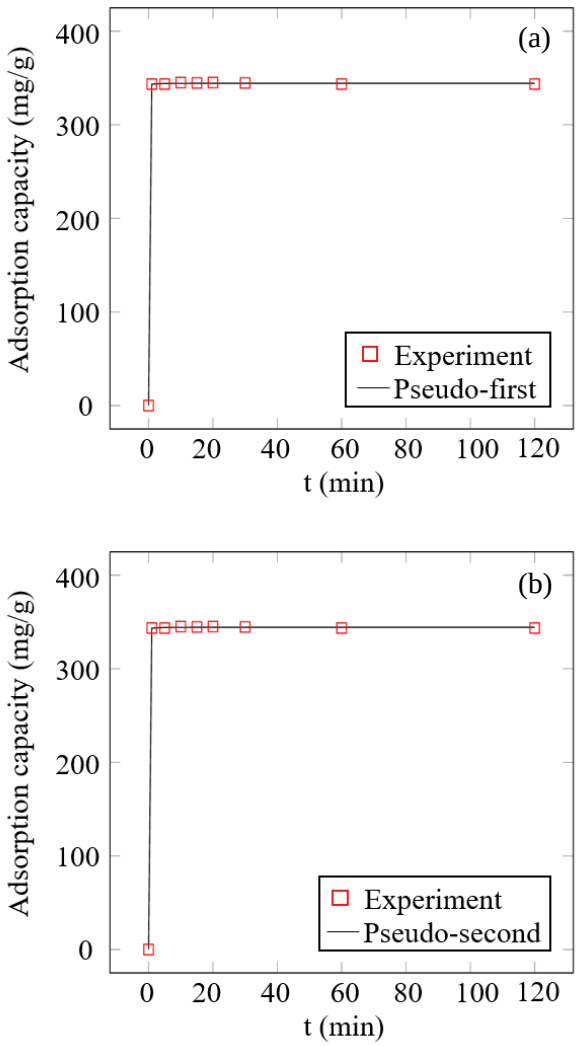

Figure 8 Kinetic plot obtained from (a) pseudo-first order model, (b) pseudo-second order model.

Table 4 Isotherm parameters for the adsorption of MB onto Na-bentonite at different temperatures.

Isotherm	Parameters	T (K)				
		308.15	313.15	318.15	323.15	328.15
	q_m (mg/g)	398.28	410.5	415.88	443.34	465.28
Langmuir	K_a	0.187	0.18	0.289	0.235	0.654
	χ^2	1.41	0.32	0.11	0.42	0.97
	K_F	303.55	282.8	321.3	286.2	337.19
Freundlich	n	21.31	16.19	22.14	12.49	17.16
	χ^2	2.97	1.56	0.93	2.26	1.36

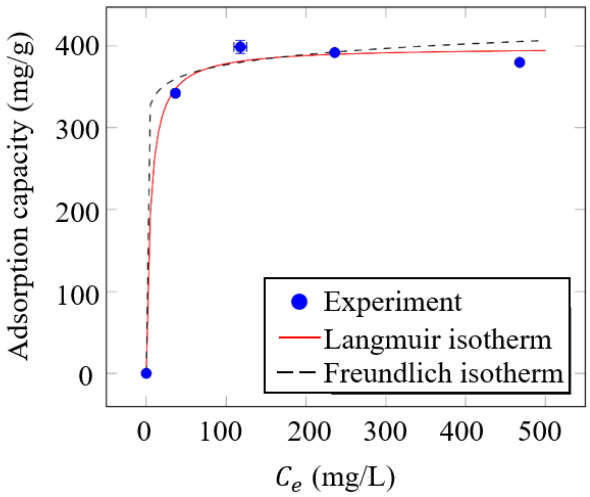

Figure 9 Plot of Langmuir and Freundlich isotherms for adsorption of MB solution onto Na-bentonite.

3.4 Isotherm

Analysis of isotherm data is implemented for design purposes. Two equilibrium isotherms were investigated: Langmuir [49] and Freundlich [50]. First, adsorption of MB solution can be described using theoretical Langmuir isotherm. It is one of the common isotherms describing adsorption of solute molecules from solution. The assumption for this model is that adsorption occurs only on the specific and uniform adsorption sites and adsorbate molecules do not interact with each other. Langmuir isotherm is given by [49]:

$$q_e = \frac{q_m K_a C_e}{1 + K_a C_e} \quad (10)$$

Where q_e is the adsorption capacity at equilibrium (mg/g), C_e is equilibrium concentration (mg/L), q_m is maximum monolayer adsorption capacity (mg/g), and K_a is the adsorption equilibrium constant (L/mg). Similarly, non-linear curve fitting, a mathematical technique, was used to determine parameters of isotherms since there is no need to transform non-linear equations into linear forms and it has similar error structure compared to other fitting isotherm methods. In order to determine the best parameters, minimization of error (χ^2) was used as given by:

$$\chi^2 = \sum_{i=1}^{N} \frac{\left(q_{e,exp} - q_{e,pre}\right)^2}{q_{e,pre}} \quad (11)$$

Where N is the number of experimental data, $q_{e,pre}$ is adsorption capacity obtained from prediction of isotherm (mg/g), and $q_{e,exp}$ is adsorption capacity at equilibrium (mg/g) obtained from experiments. Figure 9 shows the non-linear relation of Langmuir isotherm and the corresponding parameters of q_m, K_a and χ^2 are presented in Table 4. It appears that the prediction of q_e using Langmuir isotherm was able to match experimental data. This was consistent with the lower value of χ^2 in Table 4 suggesting that Langmuir isotherm provided a good fit to the experimental data. It can be explained that Na-bentonite is a homogeneous monolayer active site for MB adsorption. Further study was also investigated to examine the favorability of adsorption using the separation factor R_L given by the following equation [51]:

$$R_L = \frac{1}{1 + K_a C_i} \quad (12)$$

Isotherm can be favorable ($0 < R_L < 1$), reversible ($R_L = 0$), linear ($R_L = 1$), and unfavorable ($R_L > 1$). From the calculation, all values of R_L were 0-1 and reached 0 as C_i increased, indicating that adsorption of MB solution onto the Na-bentonite is favorable. Second, adsorption isotherm can be alternatively described by Freundlich isotherm. It is an empirical isotherm used for adsorption from dilute solutions and is able to describe multi-layer adsorption. Freundlich isotherm can be expressed by the following equation [50]:

$$q_e = K_F C_e^{1/n} \quad (13)$$

Where K_F and n are empirical constants. Figure 9 shows the non-linear relation of Freundlich isotherm and the corresponding parameters K_F, n and χ^2 are also displayed in Table 4. The results showed that the calculated q_e using Freundlich isotherm was not able to match experimental data due to the relatively high value of χ^2. Further analysis revealed that the maximum adsorption capacity q_m of Na-bentonite for the removal of MB was 465.28 mg/g indicating the excellent adsorption capacity compared to other clay based for MB removal as presented in Table 5.

3.5 Thermodynamic studies

Analysis thermodynamic studies are another important aspect for an adsorption process because they can be used to indicate spontaneity of the process under study through the change in Gibb's free energy (ΔG^o). At a given temperature, reactions occur spontaneously if the change in Gibb's free energy is a negative value. The change in Gibb's free energy can be determined from both the change in enthalpy (ΔH^o) and entropy (ΔS^o) or it can be calculated using the adsorption equilibrium constant K_a^o as given by the following equation:

$$\Delta G^o = -RT\ln K_a^o \quad (14)$$

Where ΔG^o is the change in Gibb's free energy (kJ/mol), R is the gas constant (8.314×10^{-3} kJ/mol·K), and T represents the absolute temperature (K), and K_a^o is the rate constant obtained from isotherms. It is noted that K_a^o is a dimensionless form of K_a so it requires conversion as given by:

$$K_a^o = K_a(\text{L/mg})\times1000(\text{mg/g})\times MW_{MB}(\text{g/mol})\times C^o(\text{mol/L}) \quad (15)$$

Where MW_{MB} is the molecular weight of MB (319.85 g/mol) and C^o is the standard state concentration (mol/L). Another relationship between K_a^o and the change in enthalpy (ΔH^o) is given by [20]:

Table 5 The maximum monolayer adsorption capacity of other clay based adsorbents.

Adsorbents	q_m (mg/g)	References
Bentonite with plasma-surface modification	303	Şahin et al. [21]
Bentonite modified with $CaCO_3$	120	Zhang et al. [52]
Organo-bentonite	321	Bergaoui et al. [53]
Nano-porous modified Na-bentonite	294	Moradi et al. [54]
EDTA-modified bentonite	160	De Castro et al. [55]
Nanocomposite modified bentonite	312.51	Meng et al. [22]
Surfactant-modified bentonite	36.19	Balarak et al. [23]
Na-Bentonite	465.28	This study

Table 6 Thermodynamic parameters for adsorption of MB on Na-bentonite at different temperatures

T(K)	ΔG^o (kJ/mol)	ΔH^o (kJ/mol)	ΔS^o (kJ/molK)
308.15	-28.18		
313.15	-28.54		
318.15	-30.24	46.99	0.24
323.15	-30.16		
328.15	-33.42		

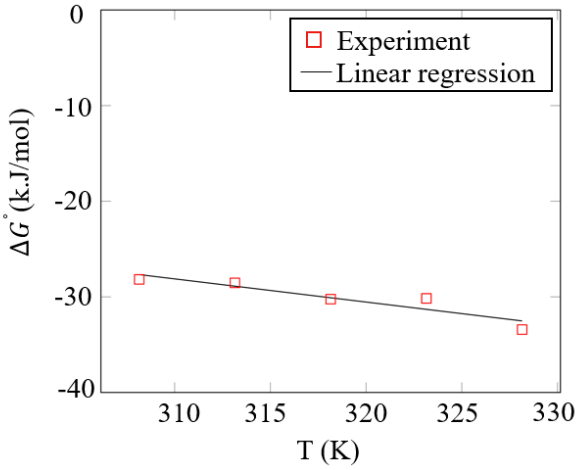

Figure 10 Thermodynamic plot of ΔG^o and T for determination of thermodynamic properties.

$$\frac{d\ln K_a^o}{dT} = \frac{\Delta H^o}{RT^2} \quad (16)$$

After integrating Eq. (16), the relationship between K_a^o and ΔH^o can be obtained,

$$\ln K_a^o = -\frac{\Delta H^o}{RT} + C \quad (17)$$

Where C is a constant value. Then, Eq. (17) is rearranged and it can be given by:

$$-RT\ln K_a^o = \Delta H^o - CRT \quad (18)$$

Eq. (18) is equivalent to the following equation:

$$\Delta G^o = \Delta H^o - T\Delta S^o \quad (19)$$

After plotting ΔG^o or $-RT\ln K_a^o$ against temperature, a linear relationship is expectedly obtained. The values of ΔS^o and ΔH^o are also calculated from the slope and intercept of the plot. The results showed that calculated ΔG^o from 35°C to 55°C were all negative, indicating that adsorption of MB solution onto Na-bentonite is feasible and spontaneous in nature. Further analysis of the change of enthalpy (ΔH^o) and entropy (ΔS^o) was performed using the linear relationship as presented in Eq. (18). Figure 10 shows the thermodynamic plot between ΔG^o versus T to calculate ΔH^o and ΔS^o. The corresponding ΔH^o and ΔS^o obtained from the intercept and slope of the plot were equal to $+46.99$ kJ/mol and $+0.24$ kJ/mol·K as presented in Table 6. Positive ΔH^o indicates that the adsorption under study is an endothermic reaction and it becomes more favorable at higher temperatures. This is in good agreement with the results in the previous section on the effect of temperature, where the adsorption capacity increases with temperature. Regarding ΔS^o, the positive value indicates the affinity of the Na-bentonite for MB solution and an increase in randomness at the solid-solution interface.

3.6 Surrogate-based models

Typically, the MB adsorption onto Na-bentonite depends on several factors including initial MB concentration, pH, contact time, and temperature. However, the previous section investigated only one factor at a time, while other factors were fixed. This could neglect the interactions among all factors. To handle such a problem, surrogate-based modeling though design of an experiment is commonly used. The development of the surrogate-based model was performed using the polynomial approximation to evaluate the effects of factors and their interactions on the adsorption capacity. The sampling method for adsorption of MB solution onto Na-bentonite was performed through full factorial design with 3 factors and 3 levels. The contact time for the adsorption was not considered in this case because MB solution was rapidly adsorbed onto Na-bentonite at the initial stage of the process based on the initial investigation. Figure 11 shows the plot between the adsorption capacity obtained from experimental data (x-axis) and from a calculation using the surrogate-based model (y-axis). Apparently, all values were close to the identity line or line of equality ($y = x$) indicating that the adsorption capacity obtained from the surrogate-based model was in good agreement with experimental data. The response of the surrogate model $\hat{y}(x)$ at defined ranges x can be efficiently predicted using Eq. (20).

$$\hat{y}(x) = 1.56 + 1.31x_1 - 14.7x_2 + 1.20x_3 + 0.18x_1x_2 + 0.029x_2x_3 + 0.0018x_1x_3 - 0.033x_1^2 + 0.27x_2^2 - 0.0012x_3^2 \quad (20)$$

Where $\hat{y}(x)$ is the predicted response (adsorption capacity, mg/g), and x_1, x_2, and x_3 are process variables i.e. temperature, initial pH and initial MB concentration, respectively.

The corresponding coefficients of the surrogate-based model and the coefficient of determination R^2 are shown in Table 7. The results showed that R^2 value of 0.987 indicated that the developed model could capture 98.7% of the data variation, and 1.3% of the total variations were not explained by the model. It is noted that R^2 should not be below 0.75. Additionally, the adjusted coefficient of determination (adjusted $R^2 = 0.97$) indicated exceptionally good agreement between the experimental data and model prediction. Table 7 also shows a statistical analysis of each

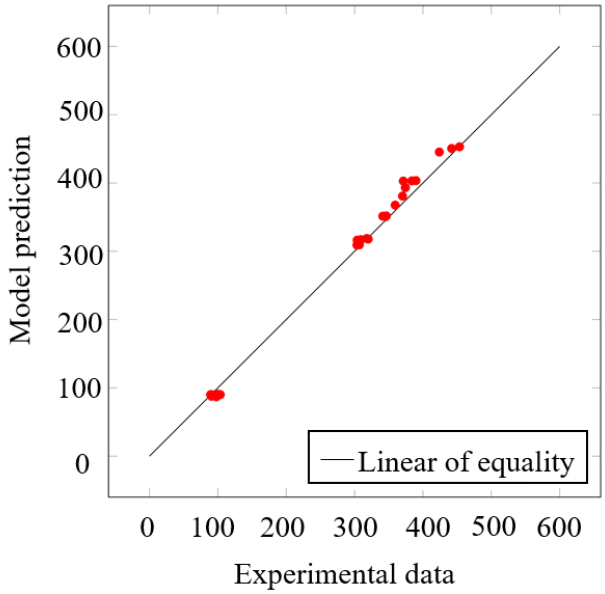

Figure 11 Adsorption capacity at different operating conditions observed in the experiment versus model prediction.

Table 7 Coefficient of the surrogate-based model and statistical analysis

Factor	Coefficient	P-value
Constant term	1.56	0.99
x_1	1.31	0.85
x_2	-14.7	0.11
x_3	1.20	1.39×10^{-12}
x_1x_2	0.18	0.15
x_2x_3	0.029	1.12×10^{-7}
x_1x_3	0.0018	0.28
x_1^2	-0.033	0.66
x_2^2	0.27	0.55
x_3^2	-0.0012	2.16×10^{-19}
R^2	0.987	
Adjusted R^2	0.97	

coefficient term in the surrogate-based model. It is important to note that the significance of each coefficient term is indicated by P values. The results showed that the P-values of x_3, x_2, x_3, and x_3^2 terms were below 5%. Statistically, the low P-value (below 5%) of each coefficient indicates that the corresponding coefficient term is significant and have significant effects on the adsorption capacity. The other terms have no significant effect on adsorption capacity since the P-value is higher than 5%.

The response surface was plotted to study the interaction among factors. The effect of temperature and initial pH on the adsorption capacity at a constant initial MB concentration is shown in Figure 12(a). The adsorption capacity was observed to increase significantly with an increase in initial pH compared to that of temperature. There is a net positive interactive effect between temperature and initial pH and this probably results from interaction effects of surface charge and endothermic reaction. The interactive effect of temperature and initial MB concentration on adsorption capacity at a constant initial pH is shown in Figure 12(b). Overall, a positive interactive effect between temperature and initial MB concentration was observed from Eq. (20), indicating that the adsorption capacity increased with an increase in the temperature and initial MB concentration. However, a trade-off or interplay was also observed at the higher initial concentration. As the initial MB concentration increased, the adsorption capacity decreased because of the limited number

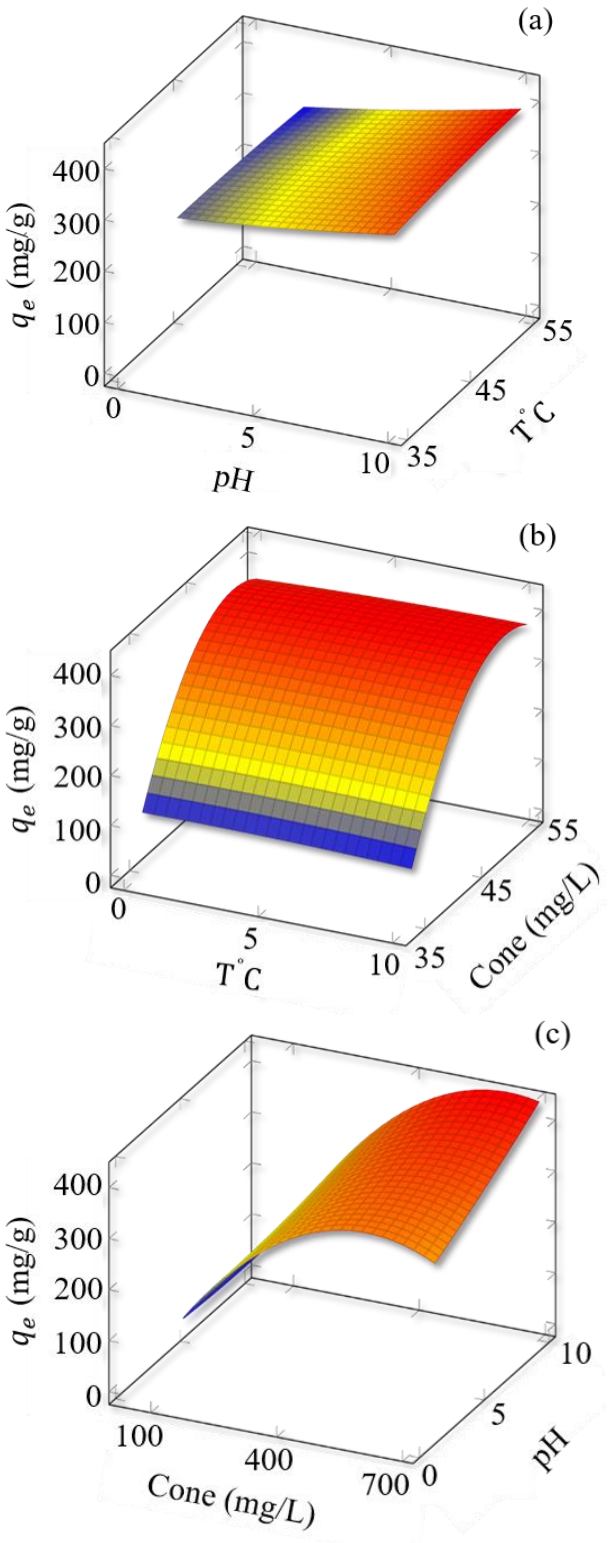

Figure 12 Response surface plot of (a) initial pH and temperature (b) temperature and initial concentration (c) initial concentration and initial pH on adsorption capacity.

of adsorbent active sites. Finally, the interactive effect of initial MB concentration and initial pH on the adsorption capacity at a constant temperature is shown in Figure 12(c). The plot or trend in Figure 12(c) is similar to that of Figure 12(b). There is a net positive interactive effect indicating that the adsorption capacity increases with an increase in the initial MB concentration and initial pH but at a certain initial MB concentration (above 500 mg/L), the adsorption capacity decreases as the initial MB concentration increases.

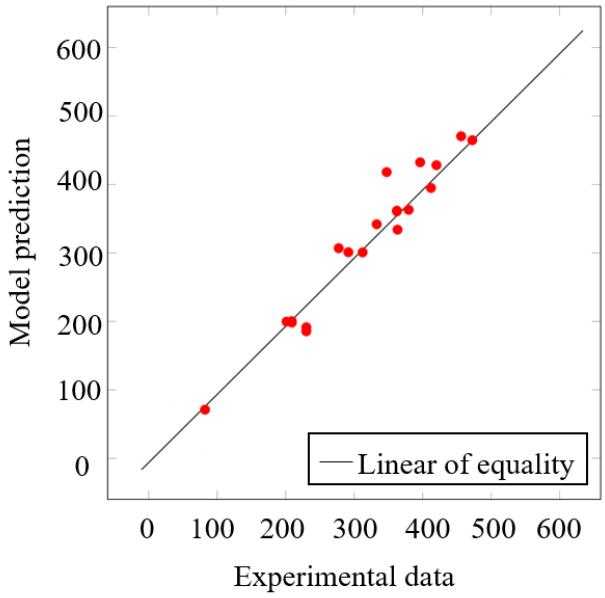

Figure 13 Adsorption capacity at different operating conditions for model validation.

After the development of the surrogate-based model, it is important to validate the model using a different set of data. Another set of experiment was conducted at different operating conditions. Figure 13 shows the plot between the adsorption capacity obtained from the different set of experimental data and from model prediction. It was found that most of the values were close to the line of equality ($y = x$), with the average percent error of 5.6% suggesting good agreement between experimental data and model prediction. This can confirm the adequacy of the surrogate-based model. Once the surrogate-based model was developed and validated, it could be used to optimize the operating condition using the numerical optimization technique. The optimal conditions for the adsorption of MB solution using Na-bentonite were found at a pH of 10, a temperature of 55°C and initial MB concentration of 634 mg/L. The optimal conditions obtained from numerical optimization required validating the results. Again, the experiments were conducted using the optimal conditions and the average adsorption capacity is 438.13 ± 5.21 mg/g. The results showed a percent difference of 4.60% (4.71% percent error). This shows good agreement between the experimental data and model prediction, confirming that the surrogate-based model can be used to optimize the operating conditions. Note that small discrepancy is attributable to a residual error in Eq. (3). Measuring the variation in the measured data unexplained by the surrogate-based model [56] and a rounding error.

4. Conclusions

The results of this study suggest that Na-bentonite is an effective adsorbent for removing cation dye (MB) from water. Na-bentonite is widely available, environmentally friendly and cheap, which makes it viable for as an adsorbent used to treat the large volume of dye wastewater. The adsorption conditions such as pH, temperature, and initial MB concentration were found to have effects on adsorption capacity. Regarding kinetics and isotherm, the pseudo-first order, pseudo-second order and Langmuir models were a better fit with the experimental data. The maximum adsorption capacity obtained from the Langmuir model also increased with an increase in temperature. The changes in enthalpy and entropy were all positive indicating that the adsorption of MB onto Na-bentonite is endothermic and spontaneous. Development of the surrogate-based model was another contribution in this study since it can be used to study the interaction of operating factors and to determine the optimal conditions. Predictions of the adsorption capacity were close to the measured data from the experiments suggesting the adequacy of the surrogate-based model. The optimal conditions were found at the initial concentration of 634 mg/L, a pH of 10, and a temperature of 55°C. Overall, this research has shown that Na-bentonite, which is a low cost, abundance, and locally available is an effective adsorbent for MB removal.

5. Acknowledgements

The project is funded in part by the Thailand Research Fund (TRF), under Grant No. MRG6080255. The authors wish to thank the Department of Chemical Engineering, Ubon Ratchathani University for research facilities.

6. References

[1] Koswojo R, Utomo R, Ju Y, Ayucitra A, Soetaredjo F, Sunarso J, et al. Acid green 25 removal from wastewater by organo-bentonite from pacitan. Appl Clay Sci. 2010;48(1):81-6.

[2] McMullan G, Meehan C, Conneely A, Kirby N, Robinson T, Nigam P, et al. Microbial decolourisation and degradation of textile dyes. Appl Microbiol Biotechnol. 2001;56(1):81-7.

[3] Sekuljica N, Prlainovic N, Stefanovic A, Zuza MG, Cickaric D, Mijin D, et al. Decolorization of anthraquinonic dyes from textile effluent using horseradish peroxidase: optimization and kinetic study. Sci World J. 2015;1-12.

[4] Metivier-Pignon H, Faur-Brasquet C, Cloirec PL. Adsorption of dyes onto activated carbon cloths: approach of adsorption mechanisms and coupling of acc with ultrafiltration to treat coloured wastewaters. Separ Purif Tech. 2003;31(1):3-11.

[5] Jeff P. Colour in textile effluents the origins of the problem. J Soc Dyer Colourists. 1994;110(4):131-3.

[6] Gupta VK, Suhas Ali I, Saini VK. Removal of rhodamineB, fast green, and methylene blue from wastewater using red mud, an aluminum industry waste. Ind Eng Chem Res. 2004;43(7):1740-7.

[7] El-Latif MA, Ibrahim A, El-Kady M. Adsorption equilibrium, kinetics and thermodynamics of methylene blue from aqueous solutions using biopolymer oak sawdust composite. J Am Sci. 2010;6(6):267-83.

[8] Sen T, Afroze S, Ang HM. Equilibrium, kinetics and mechanism of removal of methylene blue from aqueous solution by adsorption onto pine cone biomass of pinus radiata. Water Air Soil Pollut. 2011;218(1):499-515.

[9] Dharupaneedi SP, Nataraj SK, Nadagouda M, Reddy KR, Shukla SS, Aminabhavi TM. Membrane-based separation of potential emerging pollutants. Separ Purif Tech. 2019;210:850-66.

[10] Jain A, Gupta V, Bhatnagar A, Suhas, B. Utilization of industrial waste products as adsorbents for the removal of dyes. J Hazard Mater. 2003;101(1):31-42.

[11] Forgacs E, Cserhati T, Oros G. Removal of synthetic dyes from wastewaters: a review. Environ Int. 2004;30(7):953-71.

[12] Aksu Z. Application of biosorption for the removal of organic pollutants: a review. Process Biochem. 2005;40(3):997-1026.

[13 Gisi SD, Lofrano G, Grassi M, Notarnicola M. Characteristics and adsorption capacities of low-cost sorbents for wastewater treatment: A review. Sustain Mater Tech. 2016;9:10-40.

[14] Han X, Wang W, Ma X. Adsorption characteristics of methylene blue onto low cost biomass material lotus leaf. Chem Eng J. 2011;171(1):1-8.
[15] Kumar PS, Ramalingam S, Senthamarai C, Niranjanaa M, Vijayalakshmi P, Sivanesan S. Adsorption of dye from aqueous solution by cashew nut shell: Studies on equilibrium isotherm, kinetics and thermodynamics of interactions. Desalination. 2010;261(1):52-60.
[16] Ngulube T, Ray Gumbo J, Masindi V, Maity A. An update on synthetic dyes adsorption onto clay based minerals: a state-of-art review. J Environ Manag. 2017;191:35-57.
[17] Aghdasinia H, Asiabi HR. Adsorption of a cationic dye (methylene blue) by Iranian natural clays from aqueous solutions: equilibrium, kinetic and thermodynamic study. Environ Earth Sci. 2018;77:1-14.
[18] Liu Y, Kang Y, Mu B, Wang A. Attapulgite/ bentonite interactions for methylene blue adsorption characteristics from aqueous solution. Chem Eng J. 2014;237:403-10.
[19] Al- Asheh S, Banat F, Abu- Aitah L. The removal of methylene blue dye from aqueous solutions using activated and non- activated bentonites. Adsorption Sci Tech. 2003;21(5):451-62.
[20] Hong S, Wen C, He J, Gan F, Ho Y. Adsorption thermodynamics of methylene blue onto bentonite. J Hazard Mater. 2009;167(1):630-3.
[21] Şahin O, Kaya M, Saka C. Plasma-surface modification on bentonite clay to improve the performance of adsorption of methylene blue. Appl Clay Sci. 2015;116-117:46-53.
[22] Meng B, Guo Q, Men X, Ren S, Jin W, Shen B. Preparation of modified bentonite by polyhedral oligomeric silsesquioxane and sodium dodecyl sulfate in aqueous phase and its adsorption property. Mater Lett. 2019;253:71-3.
[23] Balarak D, Bazzi M, Shehu Z, Chandrika K. Application of surfactant-modified bentonite for methylene blue adsorption from aqueous solution. Orient J Chem. 2020;36(2):293-9.
[24] Queipo N, Haftka R, Shyy W, Goel T, Vaidyanathan R, Tucker P. Surrogate- based analysis and optimization. Progr Aero Sci. 2005;41(1):1-28.
[25] McBride K, Sundmacher K. Overview of surrogate modeling in chemical process engineering. Chem Ing Tech. 2019;91:228-39.
[26] Wawrzkiewicz M, Wisniewska M, Gunko V. Application of silica alumina oxides of different compositions for removal of C. I. reactive black 5 dye from wastewaters. Adsorption Sci Tech. 2017;35(5-6):448-57.
[27] Budsaereechai S, Kamwialisak K, Ngernyen Y. Adsorption of lead, cadmium and copper on natural and acid activated bentonite clay. Eng Appl Sci Res. 2012:17(5):800-10.
[28] Rostami E, Norouzbeigi R, Rahbar A. Thermal and chemical modification of bentonite for adsorption of an anionic dye. Adv Environ Tech. 2018;4(1):1-12.
[29] Leite I, Soares A, Carvalho L, Raposo C, Malta O, Silva S. Characterization of pristine and purified organo bentonites. J Therm Anal Calorimetry. 2010;100(2):563-9.
[30] Madejova J. FTIR Techniques in clay mineral studies. Vib Spectros. 2003;31(1):1-10.
[31] Xu X, Ding Y, Qian Z, Wang F, Wen B, Zhou H, et al. Degradation of poly (ethylene terephthalate) / clay nanocomposites during melt extrusion: Effect of clay catalysis and chain extension. Polymer Degrad Stabil. 2009;94(1):113-23.
[32] Xu P, Xu T, Lu J, Gao S, Hosmane NS, Huang B, et al. Visible-light-driven photocatalytic S- and C- codoped meso/nanoporous TiO_2. Energ Environ Sci. 2010;3:1128-34.
[33] Ainane T, Khammour F, Talbi M, Elkouali M. A novel bio-adsorbent of mint waste for dyes remediation in aqueous environments: study and modeling of isotherms for removal of methylene blue. Orient J Chem. 2014;30(3):1183-9.
[34] Naswir M, Arita S, Marsi M, Salni S. Characterization of bentonite by XRD and SEM- EDS and use to increase pH and color removal, Fe and organic substances in peat water. J Clean Energ Tech. 2013;1(4):313-7.
[35] Elkady M, Ibrahim AM, El-Latif M. A. Assessment of the adsorption kinetics, equilibrium and thermodynamic for the potential removal of reactive red dye using eggshell biocomposite beads. Desalination. 2011;278(1):412-23.
[36] Liu Z, Zhou S. Adsorption of copper and nickel on Na-bentonite. Process Saf Environ Protect. 2010;88(1):62-6.
[37] Gouza A, Fanidi K, Saoiabi S, Laghzizil A, Saoiabi A. Effect of heat treatment on the surface properties of selected bituminous shale for cationic dye sorption. Desalination Water Treat. 2017;66;274-80.
[38] Chham A, Khouya EH, Ouman M, Abourriche A, Gmouh S, Larzek M, et al. The use of insoluble mater of Moroccan oil shale for removal of dyes from aqueous solution. Chem Int. 2018;4(1):67-77.
[39] Al-Qodah, Z. Adsorption of dyes using shale oil ash. Water Res. 2000;34(17):4295-303.
[40] Dursun A, Tepe O. Removal of chemazol reactive red 195 from aqueous solution by dehydrated beet pulp carbon. J Hazard Mater. 2011;194:303-11.
[41] Ozbay N, Yargic A, Yarbay-Sahin R, Onal E. Full factorial experimental design analysis of reactive dye removal by carbon adsorption. J Chem. 2013:1-13.
[42] Berizi Z, Hashemi S, Hadi M, Azari A, Mahvi A. The study of nonlinear kinetics and adsorption isotherm models for Acid Red 18 from aqueous solutions by magnetite nanoparticles and magnetite nanoparticles modified by sodium alginate. Water Sci Tech. 2016;74(5):1235-42.
[43] Lin J, Wang L. Comparison between linear and non-linear forms of pseudo- first- order and pseudo- second- order adsorption kinetic models for the removal of methylene blue by activated carbon. Front Environ Sci Eng China. 2009;3(3):320-4.
[44] Langergren S, Svenska BK. Zur theorie der sogenannten adsorption geloster stoffe. Veternskapsakad Handl. 1898;24(4):1-39.
[45] McKay G, Ho YS. Pseudo-second-order model for sorption processes. Process Biochem. 1999;34:451-65.
[46] Ashrafi S, Rezaei S, Forootanfar H, Mahvi A, Faramarzi M. The enzymatic decolonization and detoxification of synthetic dyes by the laccase from a soil- isolated ascomycete, paraconiothyrium variabile. Int Biodeterioration & Biodegradation. 2003;85:173-81.
[47] Maleki A, Mahvi A, Ebrahimi R, Zandsalimi Y. Study of photochemical and sono chemical processes efficiency for degradation of dyes in aqueous solution. Korean J Chem Eng. 2020;27(6):1805-10.
[48] Caliskan E, Gokturk S. Adsorption characteristics of sulfamethoxazole and metronidazole on activated carbon. Separ Sci Tech. 2010;45(2):244-55.
[49] Langmuir I. The adsorption of gases on plane surfaces of glass, mica and platinum. J Am Soc. 1918;40(9):1361-403.
[50] Freundlich HMF. Uber die adsorption in losungen. Z Phys Chem. 1907;57(1):385-470.
[51] Weber TW, Chakkravorti RK. Pore and solid diffusion models for fixed-bed adsorbers. AICHE J. 1974;20(2):228-38.
[52] Zhang HB, Chen NH, Tong ZF, Liu QF, Tang YK, Zhou ZL, et al. Adsorption of methylene blue and Congo red on bentonite modified with $CaCO_3$. Key Eng Mater. 2017;727:853-8.
[53] Bergaoui M, Nakhli A, Benguerba Y, Khalfaoui M, Erto A, Soetaredjo FE, et al. Novel insights into the adsorption mechanism of methylene blue onto organo-bentonite:

adsorption isotherms modeling and molecular simulation. J Mol Liq. 2018;272:697-707.
[54] Moradi N, Salem S, Salem A. Optimizing adsorption of blue pigment from wastewater by nano-porous modified Na-bentonite using spectrophotometry based on response surface method. Spectrochim Acta Mol Biomol Spectros. 2018;193:54-62.
[55] De Castro MLFA, Abad MLB, Sumalinog DAG, Abarca RRM, Paopasert P, de Luna. MDG Adsorption of methylene blue dye and Cu(II) ions on EDTA-modified bentonite: Isotherm, kinetic and thermodynamic studies. Sustain Environ Res. 2018;28:197-205.
[56] Subramaniam R, Ponnusamy SK. Novel adsorbent from agricultural waste (cashew NUT shell) for methylene blue dye removal: Optimization by response surface methodology. Water Resour Ind. 2015;11:64-70.